Valence Bond and von Neumann Entanglement Entropy in Heisenberg Ladders

Ann B. Kallin,[1] Iván González,[2] Matthew B. Hastings,[3] and Roger G. Melko[1]

[1]*Department of Physics and Astronomy, University of Waterloo, Ontario, N2L 3G1, Canada*
[2]*Centro de Supercomputación de Galicia, Avda. de Vigo s/n, E-15705 Santiago de Compostela, Spain*
[3]*Microsoft Research, Station Q, CNSI Building, University of California, Santa Barbara, CA, 93106*
(Dated: July 9, 2009)

We present a direct comparison of the recently-proposed valence bond entanglement entropy and the von Neumann entanglement entropy on spin 1/2 Heisenberg systems using quantum Monte Carlo and density-matrix renormalization group simulations. For one-dimensional chains we show that the valence bond entropy can be either less or greater than the von Neumann entropy, hence it cannot provide a bound on the latter. On ladder geometries, simulations with up to seven legs are sufficient to indicate that the von Neumann entropy in two dimensions obeys an area law, even though the valence bond entanglement entropy has a multiplicative logarithmic correction.

Introduction.– Entanglement has arisen as a new paradigm for the study of correlations in condensed matter systems. Measurements of entanglement between subregions, chiefly using entropic quantities, have an advantage over traditional two-point correlation functions in that they encode the total amount of information shared between the subregions without the possibility of missing "hidden" correlations [1], such as may occur in some exotic quantum groundstates. For example spin liquid states, where two-point correlation functions decay at large lengthscales, can exhibit topological order that is quantified by a "topological entanglement entropy" [2]. This and other entropic measures are typically discussed in the context of the von Neumann entanglement entropy (S^{vN}), which for a system partitioned into two regions A and B, quantifies the entanglement between A and B as

$$S_A^{\mathrm{vN}} = -\mathrm{Tr}[\rho_A \ln \rho_A]. \qquad (1)$$

Here, the reduced density matrix $\rho_A = \mathrm{Tr}_B |\psi\rangle\langle\psi|$ is obtained by tracing out the degrees of freedom of B.

The properties of S^{vN} are well-studied in quantum information theory. In interacting one-dimensional (1D) quantum systems, exact analytical results are known from conformal field theories (CFT); they show that, away from special critical points, S_A^{vN} scales as the size of the boundary between A and B. This so-called *area law* [3] is also believed to hold in many groundstates of two dimensional (2D) interacting quantum systems, although exact results are scarce [4]. This has consequences in the rapidly-advancing field of computational quantum many-body theory, where it is known for example that groundstates of 1D Hamiltonians satisfying an area law can be accurately represented by matrix product states [5]. Tensor-network states and MERA give two promising new classes of numerical algorithms [6] that may allow simulations of 2D quantum systems not amenable to quantum Monte Carlo (QMC) due to the notorious sign problem. However, these simulation frameworks are constructed to obey an area law; in order to be represented faithfully by them, a given 2D quantum groundstate must have entanglement properties also obeying the area law [4].

Unfortunately, entanglement is difficult to measure in 2D, due to the fact that QMC does not have direct access to the groundstate wavefunction $|\psi\rangle$ required in Eq. (1). In response to this, several authors [7, 8] have introduced the concept of *valence bond* entanglement entropy (S^{VB}), defined for a spin system as

$$S_A^{\mathrm{VB}} = \ln(2) \cdot \mathcal{N}_A, \qquad (2)$$

where $\mathcal{N}_A$ is the number of singlets $(|\uparrow\downarrow\rangle - |\downarrow\uparrow\rangle)/\sqrt{2}$ crossing the boundary between regions A and B. Unlike S^{vN}, S^{VB} can be accessed easily in the valence-bond basis projector QMC method recently proposed by Sandvik [9]. As demonstrated in Refs. [7, 8], S^{VB} has many properties in common with S^{vN}, in particular the relationship $S_A^{\mathrm{VB}} = S_B^{\mathrm{VB}}$, and the fact that $S_A^{\mathrm{VB}} = 0$ for regions "un-entangled" by valence bonds. A comparison of the scaling of S^{VB} for (critical) 1D spin 1/2 Heisenberg chains shows good agreement with analytical results known from CFT, however in the 2D isotropic Heisenberg model it displays a *multiplicative* logarithmic correction to the area law [7, 8]. If true also for S^{vN}, this would have negative consequences for the simulation of the Néel groundstate using tensor-network simulations.

In this paper, we compare S^{VB} calculated by valence-bond QMC to S^{vN} accessible through density-matrix renormalization group (DMRG) simulations of the Heisenberg model on N-leg ladders. For $N = 1$, the CFT central charge calculated by scaling S^{vN} shows excellent agreement to $c = 1$, whereas S^{VB} converges to $c < 1$. For $N > 1$, S^{VB} is systematically greater than S^{vN}, a trend which grows rapidly with N. An examination of entanglement defined by bipartitioning multi-leg ladders shows a logarithmic correction for the valence-bond entanglement entropy, $S^{\mathrm{VB}} \propto N \ln N$ (in agreement with Refs. [7, 8]), however for data up to $N = 7$, the von Neumann entanglement entropy convincingly shows a scaling of $S^{\mathrm{vN}} \propto N$, thus obeying the area law.

Model and Methods.– We consider the spin 1/2 Heisenberg Hamiltonian, given by $H = \sum_{\langle ij \rangle} \mathbf{S}_i \cdot \mathbf{S}_j$, where the sum is over nearest-neighbor lattice sites. Geometries

studied are 1D chains, and multi-leg ladders with length L and number of legs N. We employ two complementary numerical techniques, the valence-bond basis QMC and DMRG, both of which give *unbiased* approximations to the ground state of the Hamiltonian at zero temperature. S_A^{vN} is naturally accessible through the DMRG algorithm [10]. At each step of the algorithm, the wavefunction of the system is approximated by keeping only the states with largest coefficients in the Schmidt decomposition for a given bipartition into regions A and B $\equiv$ ∁A. To find the basis entering the Schmidt decomposition for region A, the reduced density matrix ρ_A is calculated and diagonalized, thus allowing easy calculation of Eq. (1). The truncation of the basis implies that only a lower bound for S_A^{vN} is calculated, so care must be taken to ensure that enough of the eigenvalue spectrum is included to converge S_A^{vN} to sufficient accuracy; typically the number of states required is larger than that needed to converge the energy alone. We have kept up to 1800 states per block for the largest ladders, with truncation errors under 10^{-7} in all cases.

S_A^{VB} can be calculated using the valence-bond basis QMC proposed by Sandvik [9]. The algorithm we use is the simple single-projector method, with lattice geometries constructed to match those used by DMRG. The ground state of the system is projected out by repeated application of a list of nearest-neighbor bond operators, a number of which are changed each step. The change is accepted with a probability of $2^{n_b}/2^{n_a}$ where n_a (n_b) is the number of off-diagonal operators in the current (last accepted) step. Measured quantities such as energy or S_A^{VB} are then calculated by a weighted average over all the valence bond states obtained by this procedure.

One-dimensional chain.– We consider first the case of Heisenberg chains ($N = 1$) of length L, simulating both open (OBC) and periodic (PBC) boundary conditions. The DMRG algorithm requires the regions A and B to be topologically connected, so in 1D the bipartition is defined by a site index x with sites within the interval $[1, x]$ ($[x + 1, L]$) belonging to region A (B) [thus we can label S_A by its site index, $S(x)$]. We stress that the QMC and DMRG results are on the same geometry and Hamiltonian, and reproduce the same ground state energies; Figure 1 (and subsequent figures) should be considered as exact comparisons between S^{VB} and S^{vN}.

The 1D Heisenberg model is known to be critical and thus can be mapped to a 2D classical Hamiltonian at its critical point, which can be described by CFT in the limit $L \to \infty$. To address finite-length chains one can use the conformal mappings $x \to x' = (L/\pi)\sin(\pi x/L)$ for PBC, and $x \to 2x'$ for OBC. Calculations within CFT [11] obey $S^{vN}(x) = (c/3)\ln(x') + S_1$ for PBC, and $S^{vN}(x) = (c/6)\ln(2x') + \ln(g) + S_1/2$ for OBC, where c is the central charge of the CFT, S_1 is a model-dependent constant, and g is Ludwig and Affleck's universal boundary term [12].
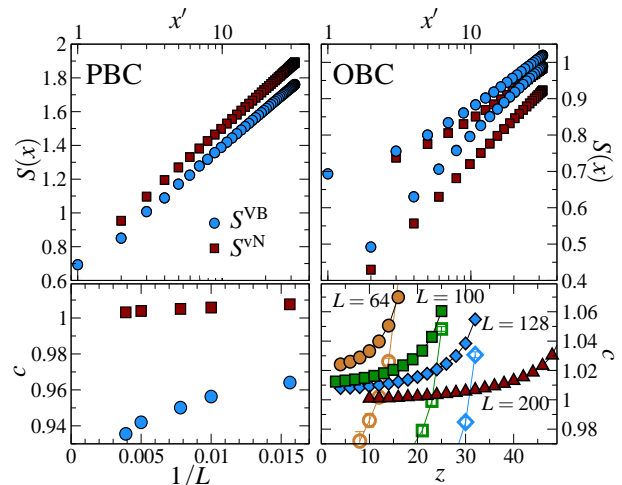

FIG. 1: (color online) Entanglement entropies for a 1D Heisenberg chain with PBC and OBC. Upper panels show the entropies as a function of the conformal distance $x' = (L/\pi)\sin(\pi x/L)$ for 100-site chains. Lower plots show the central charge c, obtained by fitting the numerical data to the CFT result, for several L. For PBC, c is calculated with the two smallest x' points removed. For OBC, the fits depend on the number of sites included, z, which we systematically decrease by removing x' data points from the *outside* ends of the chain. c is shown for S^{vN} (closed symbols) and S^{VB} (open symbols) for system sizes $L = 64$ (circles), $L = 100$ (squares), $L = 128$ (diamonds), and $L = 200$ (triangles)

Figure 1 illustrates simulation results in both cases, the left (right) panels corresponding to PBC (OBC). For PBC both S^{VB} and S^{vN} appear to fit well to the CFT result, although $S^{vN} > S^{VB}$. The regression fit for S^{vN} shows very good convergence with the central charge predicted by CFT, $c = 1$, while the fit for S^{VB} yields a lower value of c than predicted. For OBC both S^{vN} and S^{VB} split into two branches, the upper (lower) corresponding to an odd (even) number of lattice sites in A. This reflects a well-known "dimerization" effect induced by OBC [13]. Notice that contrary to the PBC case, now $S^{vN} < S^{VB}$. A regression fit of the lower branch to the form $(c/6)\ln(2x')$ (inset) shows excellent convergence of S^{vN} to the central charge predicted by CFT, $c = 1$, once finite-size effects and the proximity of the data to the open boundaries are taken into account. In contrast, S^{VB} deviates significantly from the CFT result, giving $c > 1$ when all or most data is included in the fit, changing to $c < 1$ as data closest to the open boundary is systematically excluded [14], e.g. for $z = L/2$, $c_{L\to\infty} \approx 0.85$.

Multi-leg ladders.– Moving away from the 1D chain, one can add "legs" to the lattice in a systematic way. In this case the sum over nearest neighbors is extended to neighbors along rungs as well as along legs. As noted before, DMRG imposes constraints to the subregion geometry. In multi-leg ladders we choose to sweep in a 1D path that visits first bonds sitting in rungs rather than
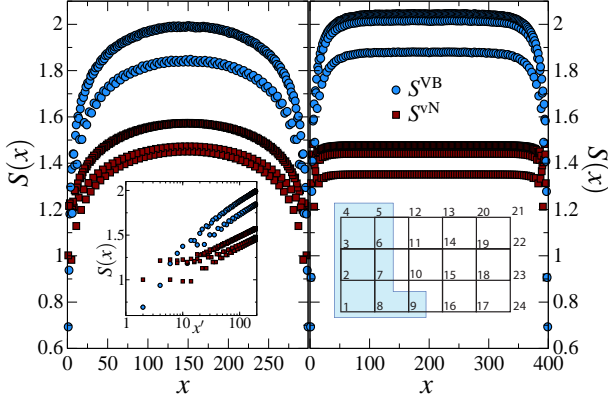
FIG. 2: (color online) Entanglement entropies for 3-leg (left) and 4-leg (right) ladder systems with OBC and 100 sites per leg. For odd-leg ladders, $S(x) \propto \ln(x')$. The left inset shows $S(x)$ as a function of the conformal distance, x', on a log scale. For even-leg ladders, $S(x \gtrsim \xi) = $ const. The right inset shows the site indexing used for multi-leg ladders where the bipartition A is shaded and labeled by $x = 9$.

FIG. 3: (color online) Entanglement entropies divided by N, for N-leg Heisenberg (filled symbols) and free-fermion (open diamonds) ladders, taken such that the region A includes $2N^2$ sites. For the Heisenberg model and large N, $S^{\mathrm{VB}} \propto N \ln N$, whereas $S^{\mathrm{vN}} \propto N$. Data for free fermions, $S^{\mathrm{vN}}_{\mathrm{ff}} \propto N \ln N$, are shown for comparison. We show data for ladders with length (sites per leg) $L = 100$ and $L = 4N$.

bonds sitting in legs (see Fig. 2). DMRG computational demands increase dramatically with the number of legs, so in this paper we restrict ourselves to ladders with OBC up to $N = 7$ legs. QMC lacks this limitation and one can go up to $N = 20$ with minimal CPU effort.

Figure 2 shows S^{vN} and S^{VB} calculated for the 3-leg and 4-leg ladder. As for the OBC 1D chain, $S^{\mathrm{VB}} > S^{\mathrm{vN}}$. Entropy shows different behavior depending on N being even or odd. Even-leg ladders have a spin-gap [15], and thus only sites within distances from the boundary between A and B *smaller* than the correlation length ξ contribute to the entanglement, yielding $S(x \gtrsim \xi) = $ const. In contrast, odd-leg ladders are gapless, and thus all sites contribute to the entanglement, yielding $S(x) \propto \ln(x')$, which follows the CFT result in analogy to the 1D case. As can be seen, $S(x)$ splits into branches, with a (quasi-)periodic structure superimposed over the main dependence on x, the period being N ($2N$) for even- (odd-) leg ladders. This reflects the periodicity of the underlying 1D path through which the algorithm sweeps, and the fact that valence bonds within the same rung are energetically favored [15]. The doubled period for odd-leg ladders is due to the same dimerization effect as in Ref. [13].

Area law in multi-leg ladders.– We can use these results to address the question of the adherence of the 2D Néel state to an area law. To do so, we define the lattice geometry such that region A is rectangular, cutting a multi-leg ladder cleanly across all legs, so that the "area" separating region A and B is equivalent to the number of legs in the ladder N. We choose the region A to contain $2N^2$ sites, to have an aspect ratio of order unity. In contrast, the entanglement entropy of a long narrow region would be dominated by the behavior of the gapless mode for odd-leg ladders. The 2:1 aspect ratio makes the region
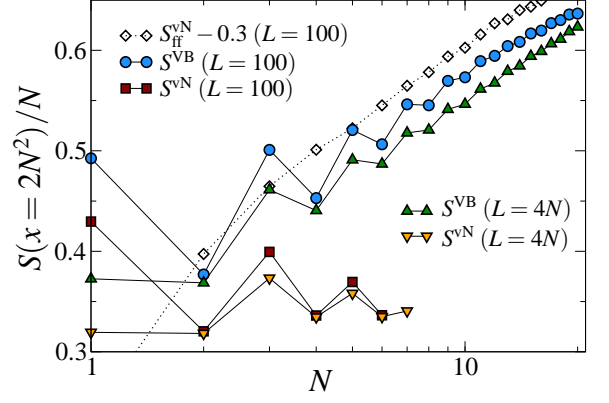
length even for all N, reducing even-odd oscillations.

Figure 3 illustrates the simulation results for N-leg ladders. Plotting $S(x)/N$ versus N on a log scale, we obtain a multiplicative logarithmic correction to the S^{VB} area law, in agreement with results from Refs. [7, 8]. However, the linear slope is *not* present in the plot of the S^{vN} data from the DMRG, which convincingly approaches a constant for large N [16]. Clearly, for S^{vN} the area law is indeed obeyed in the Néel groundstate, leading one to conclude that the multiplicative logarithmic correction occurs in S^{VB} only. One can compare S^{VB} to data obtained for free fermions, which has a well-known [17] logarithmic correction to the area law for S^{vN} (Fig. 3). In the next section, we explain S^{VB} in the context of the bond length distribution in the QMC. We note also that, contrary to the suggestion in Ref. [7], a gapless Goldstone mode will *not* give a logarithmic divergence to S^{vN} since a gapless bosonic mode in 2D obeys an area law [18]. We have also done a spin-wave calculation of S^{vN} for this system and found an area law, albeit with $S(x)/N \approx 0.2$, slightly lower than suggested for spin 1/2 in Fig. 3.

Bond Length Distribution.– Sandvik defined the bond length distribution $P(x, y)$ as the probability of a bond going from site x to site y, and found that $P(x, y) \sim |x - y|^{-p}$ with $p \approx 3$ in the Néel state [9]. This value of p gives the logarithmic divergence in S^{VB}, as can be found by directly calculating

$$S_A^{\mathrm{VB}} = \sum_{x \in A, y \in B} P(x, y) \ln(2). \qquad (3)$$

We can understand the value of p from a scaling argument similar to that in Ref. [19]. Consider the number of bonds of length l exiting a region of linear size l. For $p > 4$, this scales to zero and such a state should

have no long-range order. For $p = 4$, this number is l-independent, corresponding to a critical state ($p = 2$ is the critical power in 1D, matching the observed logarithmic behavior of S^{VB}). For $p < 2$, the bond length distribution is unnormalized, and all bonds are long, so that there is no short-range order. $p = 3$ represents a state with both long- and short-range order. There is a heuristic argument that $p = 3$ corresponds to a state with Goldstone modes: the correlation function of two spins is the probability that they lie on the same loop. This can be estimated by the Green's function of a Lévy flight with power law distributed steps with power 3, reproducing the power law decay of correlations.

Discussion.– In this paper, we have compared scaling properties of the valence bond entanglement entropy (S^{VB}) [7, 8] to the von Neumann entanglement entropy (S^{vN}) in the spin $1/2$ Heisenberg model on multi-leg ladder geometries, using QMC and DMRG simulations. In 1D, we find that S^{VB} mimics the behavior of S^{vN} closely, although it is less than S^{vN} for periodic chains, and greater than S^{vN} for open chains. In addition, fits to 1D conformal field theory, which are excellent for S^{vN} calculated via DMRG, appear to deviate significantly for S^{VB} in the large chain-size limit, approaching $c < 1$ for both boundary conditions [14].

The fact that S^{VB} can be either greater or less than S^{vN} can be understood through simple examples. Let $|(ij)(kl)...\rangle$ denote a state in which sites i, j are in a singlet, sites k, l are in a singlet, and so on. Consider an 8-site chain, with sites 1 to 4 in region A. Then, the state $|(12)(34)(56)(78)\rangle + |(14)(32)(58)(76)\rangle$ has vanishing S_A^{VB} since no bonds connect A to B, but non-vanishing $S_A^{\mathrm{vN}} \approx 0.325$. On the other hand, consider a 4-site chain, with sites 1 and 3 in region A. Then, the state $|(12)(34)\rangle + |(14)(32)\rangle$ has a maximal S_A^{VB}, equal to $2 \ln(2) \approx 1.386$, while $S_A^{\mathrm{vN}} = \ln(3) \approx 1.099$ is smaller. This second state has the maximum possible Néel order parameter: it is the equal amplitude superposition of all configurations of bonds connecting the two sublattices. Thus, it is unsurprising that states with Néel order show $S^{\mathrm{VB}} > S^{\mathrm{vN}}$, a fact which we have demonstrated numerically on multi-leg ladder systems with open boundaries.

Defining the boundary between the two entangled regions as being bipartitioned by a cut across all legs on a ladder, we have shown using DMRG that S^{vN} obeys the area law in the many-leg limit. Since DMRG can also accurately measure logarithmic size-dependencies of S^{vN} (in 1D critical systems), this suggests that simulation procedures similar to those here might enable the measurement of area-law corrections in S^{vN} as indicators of exotic phases in other models, such as those with a spinon Fermi surface [20].

The valence bond entanglement entropy harbors a multiplicative logarithmic correction for the Néel groundstate, which we have shown is caused by the valence-bond length distribution, and is not present in S^{vN}. It is clear that S^{VB} is a reasonable measurement of entanglement, readily accessible to numerical simulations in 2D and higher, and capable of reproducing the area law in some gapped groundstates [7, 8]. However, the inability of S^{VB} to provide a bound on S^{vN} (unlike other measures such as Renyi entropies), along with its discrepancies from S^{vN} in 1D critical systems and the 2D Néel state, must be taken into account in proposals to use S^{VB} for future tasks such as characterizing topological phases or studying universality at quantum phase transitions.

[1] M. M. Wolf, F. Verstraete, M. B. Hastings, and J. I. Cirac, Phys. Rev. Lett. **100**, 070502 (2008).
[2] A. Kitaev and J. Preskill, Phys. Rev. Lett. **96**, 110404 (2006); M. Levin and X.-G. Wen, *ibid.* **96**, 110405 (2006).
[3] M. Srednicki, Phys. Rev. Lett. **71**, 666 (1993).
[4] J. Eisert, M. Cramer, and M. Plenio, arXiv:0808.3773.
[5] S. Östlund and S. Rommer, Phys. Rev. Lett. **75**, 3537 (1995).
[6] F. Verstraete and J. I. Cirac, arXiv:cond-mat/0407066; F. Verstraete, M. M. Wolf, D. Perez-Garcia, and J. I. Cirac, Phys. Rev. Lett. **96**, 220601 (2006); G. Evenbly and G. Vidal, Phys. Rev. B **79**, 144108 (2009).
[7] F. Alet, S. Capponi, N. Laflorencie, and M. Mambrini, Phys. Rev. Lett. **99**, 117204 (2007).
[8] R. W. Chhajlany, P. Tomczak, and A. Wójcik, Phys. Rev. Lett. **99**, 167204 (2007).
[9] A. W. Sandvik, Phys. Rev. Lett. **95**, 207203 (2005).
[10] S. R. White, Phys. Rev. Lett. **69**, 2863 (1992); S. R. White, Phys. Rev. B **48**, 10345 (1993). See also U. Schollwöck, Rev. Mod. Phys. **77**, 259 (2005).
[11] P. Calabrese and J. Cardy, J. Stat. Mech.: Theor. Exp. P06002 (2004); H. Q. Zhou, T. Barthel, J. O. Fjaerestad, and U. Schollwoeck, Phys. Rev. A **74**, 050305(R) (2006).
[12] I. Affleck and A. W. W. Ludwig, Phys. Rev. Lett. **67**, 161 (1991).
[13] N. Laflorencie, E. S. Sorensen, M.-S. Chang, and I. Affleck, Phys. Rev. Lett. **96**, 100603 (2006).
[14] J. L. Jacobsen and H. Saleur, Phys. Rev. Lett. **100**, 087205 (2008).
[15] S. R. White, R. M. Noack, and D. J. Scalapino, Phys. Rev. Lett. **73**, 886 (1994).
[16] We note that other choices of bipartition compatible with DMRG sweeping give similar results for Fig. 3.
[17] M. M. Wolf, Phys. Rev. Lett., **96**, 010404 (2006).
[18] M. Cramer, J. Eisert, M. B. Plenio, and J. Dreissig, Phys. Rev. A **73**, 012309 (2006).
[19] B. Kozma, M. B. Hastings, and G. Korniss, Phys. Rev. Lett. **95**, 018701 (2005).
[20] D. N. Sheng, O. I. Motrunich, and M. P. A. Fisher, Phys. Rev. B **79**, 205112 (2009).